ACS Chemical Neuroscience

Research Article

pubs.acs.org/chemneuro

Rotenone Inhibits Autophagic Flux Prior to Inducing Cell Death

Burton J. Mader,[†,‡,∥] Violetta N. Pivtoraiko,[†,§,∥] Hilary M. Flippo,[†] Barbara J. Klocke,[§] Kevin A. Roth,[§] Leandra R. Mangieri,[†] and John J. Shacka*[,†,‡]

[†]Department of Pathology, Neuropathology Division, University of Alabama at Birmingham, Birmingham, Alabama, United States
[‡]Birmingham VA Medical Center, Birmingham, Alabama, United States

ABSTRACT: Rotenone, which selectively inhibits mitochondrial complex I, induces oxidative stress, α-synuclein accumulation, and dopaminergic neuron death, principal pathological features of Parkinson's disease. The autophagy−lysosome pathway degrades damaged proteins and organelles for the intracellular maintenance of nutrient and energy balance. While it is known that rotenone causes autophagic vacuole accumulation, the mechanism by which this effect occurs has not been thoroughly investigated. Treatment of differentiated SH-SY5Y cells with rotenone (10 μM) induced the accumulation of autophagic vacuoles at 6 h and 24 h as indicated by Western blot analysis for microtubule associated protein-light chain 3-II (MAP-LC3-II). Assessment of autophagic flux at these time points indicated that autophagic vacuole accumulation resulted from a decrease in their effective lysosomal degradation, which was substantiated by increased levels of autophagy substrates p62 and α-synuclein. Inhibition of lysosomal degradation may be explained by the observed decrease in cellular ATP levels, which in turn may have caused the observed concomitant increase in acidic vesicle pH. The early (6 h) effects of rotenone on cellular energetics and autophagy−lysosome pathway function preceded the induction of cell death and apoptosis. These findings indicate that the classical mitochondrial toxin rotenone has a pronounced effect on macroautophagy completion that may contribute to its neurotoxic potential.

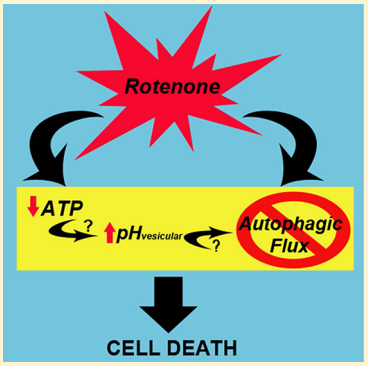

KEYWORDS: *Rotenone, autophagy, lysosome, cell death, Parkinson's disease, SH-SY5Y*

Parkinson's disease (PD) is an age-related neurodegenerative disorder that affects upward of 1−2% of persons age 60 or older and is characterized pathologically by the loss of substantia nigra dopaminergic neurons and accumulation of intracellular protein inclusions termed Lewy bodies.[1] Oxidative stress and a decreased capacity of neurons to degrade α-synuclein (α-syn), a protein reportedly involved in vesicular dopamine release and the major component of Lewy bodies, are believed to be major contributors to Lewy body formation and neurodegeneration in PD.[2]

A decreased function of complex I of the mitochondrial electron transport chain is reported in the substantia nigra of PD patients[1] that may lead to the generation of oxidative stress and a decrease in ATP production. One mechanism by which cells compensate for this disruption in energy balance is through stimulation of the autophagy−lysosome pathway (ALP), which shuttles outlived and/or damaged proteins and organelles to the lysosome for their pH-dependent degradation and recycling.[3−5] In macroautophagy, a subset of the ALP, double-membraned autophagic vacuoles shuttle cargo destined for degradation to lysosomes. Increased numbers of autophagic vacuoles are detected in several human Lewy body diseases including PD and dementia with Lewy bodies[6−8] as well as in animal models of PD.[9] Moreover, the ALP is believed to be the main route for degradation of α-syn oligomers and aggregates, further implicating its dysfunction in PD pathology.[10]

Exposure to environmental pesticides such as rotenone, a selective inhibitor of complex I of the mitochondrial electron transport chain, is associated with an elevated risk of developing PD and is used experimentally to model PD pathophysiology.[11,12] Rotenone induces neurodegeneration and neuron death in association with caspase activation,[13] and causes α-syn accumulation in experimental models of PD.[11,14] Moreover, rotenone-induced oxidative stress reportedly induces post-translational modifications of α-syn,[15] which are thought to promote its aggregation and toxicity.[16,17]

Rotenone has also been shown in several studies to cause accumulation of autophagic vacuoles,[8,18−21] as a likely response to inhibition of mitochondrial function and generation of oxidative stress. However, it is not entirely clear if rotenone-induced accumulation of autophagic vacuoles results from either an increased induction of macroautophagy or from the inhibition of macroautophagy completion, which requires functional fusion of autophagic vacuoles with lysosomes.[3] Such information may be important for designing rational therapeutics that attenuate PD-associated neuronal dysfunction, in part through their maintenance of ALP function. Thus, the goal of this study was to delineate the mechanism by which autophagic vacuoles accumulate in cultured neuronal cells following treatment with an acute, death-inducing concentration of rotenone.

Received: August 31, 2012
Accepted: September 13, 2012
Published: September 13, 2012

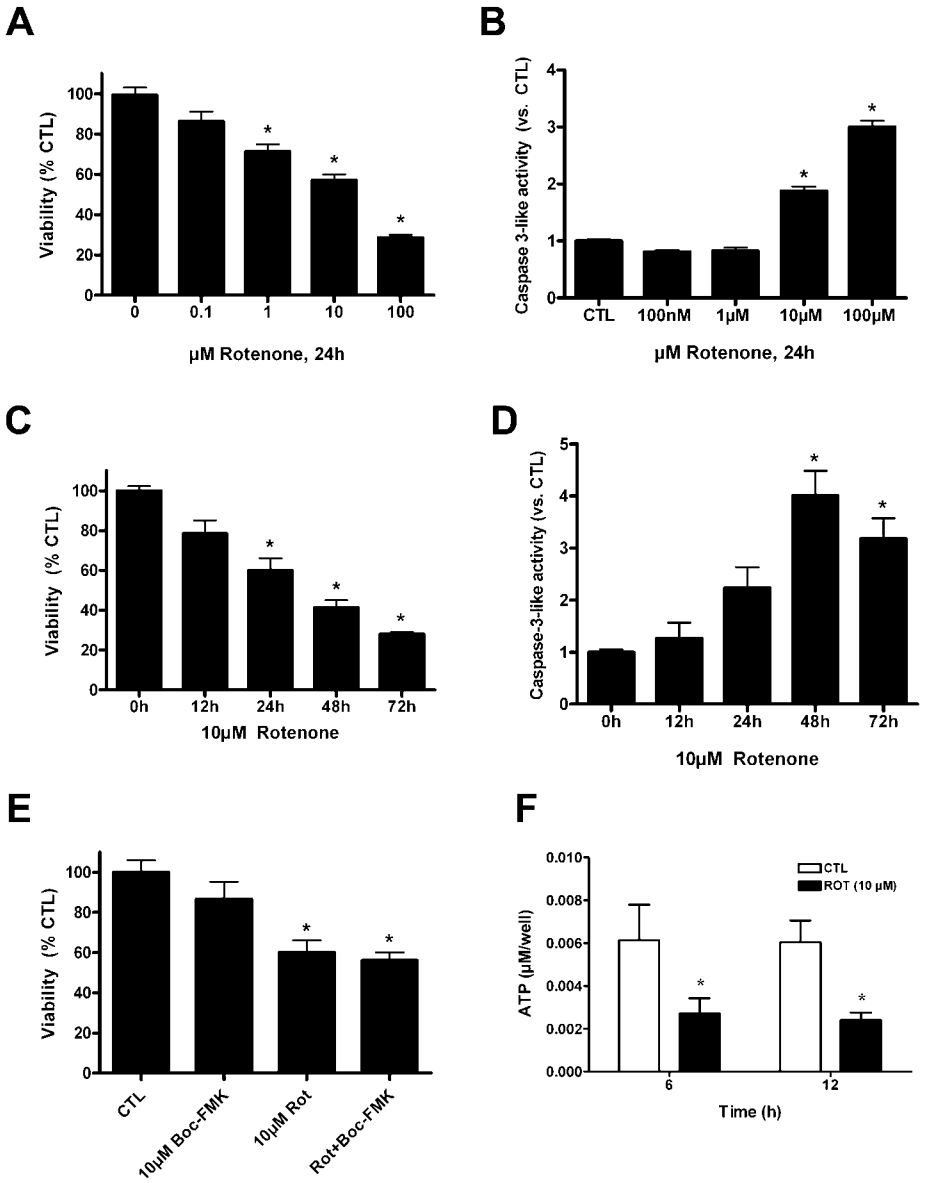

Figure 1. Rotenone induced SH-SY5Y cell death and caspase-3-like activity are concentration- and time-dependent. Rotenone induced a concentration-dependent decrease in cell viability (A) and increase in caspase-3-like activity (B), observed 24 h after treatment. 10 μM rotenone induced a time-dependent decrease in SH-SY5Y cell viability (C) that was accompanied by an increase in caspase-3-like activity (D) at 48 and 72 h of treatment. Complete inhibition of rotenone-induced caspase-3-like activity (not shown) with the broad caspase inhibitor Boc-FMK (Boc-Asp-FMK) does not attenuate the decrease in cell viability after 48 h treatment with 10 μM rotenone (E). Rotenone (10 μM) induced a significant decrease in cellular ATP levels (μM/well) at 6 and 12 h after treatment compared to CTL (F). Results represent mean ± standard deviation, and experiments were repeated independently at least three times with similar results. *$p < 0.05$ vs 0 μM rotenone CTL (A, B, E, F); *$p < 0.05$ vs 0 h rotenone (C, D).

RESULTS AND DISCUSSION

It is well established that rotenone disrupts the ALP. However, the cause of autophagic vacuole accumulation following rotenone treatment has not been carefully investigated. The purpose of this study was to assess the manner by which rotenone, a potent mitochondrial toxin that is used as an experimental model of PD, affects accumulation of autophagic vacuoles using a neuroblastoma cell line (SH-SY5Y) that was differentiated to a neuronal phenotype. We first assessed cell death, apoptosis, and energetics following treatment with rotenone. Next, using a death-inducing concentration of rotenone, we assessed autophagic flux to determine the manner by which autophagic vacuoles accumulate. We next assessed vesicular acidification and the integrity of lysosomal membranes to determine the potential for acidic vesicle dysfunction to contribute to changes observed in autophagic flux. Finally, we correlated these observed effects of rotenone on macroautophagy by assessing relative levels of a lysosomal membrane marker and a transcription factor that is responsible for its stress-induced up-regulation.

Rotenone-Induced Neuronal Cell Death and Apoptosis. In retinoic acid-differentiated SH-SY5Y cells, rotenone induced concentration and time-dependent cell death (Figure 1A, C). A decrease in cell viability was observed beginning at 24 h of 10 μM rotenone treatment. About a 50% decrease in SH-SY5Y cell viability was observed after 48 h of rotenone treatment, which progressed to 70% by 72 h (Figure 1C).

dx.doi.org/10.1021/cn300145z | ACS Chem. Neurosci. 2012, 3, 1063−1072

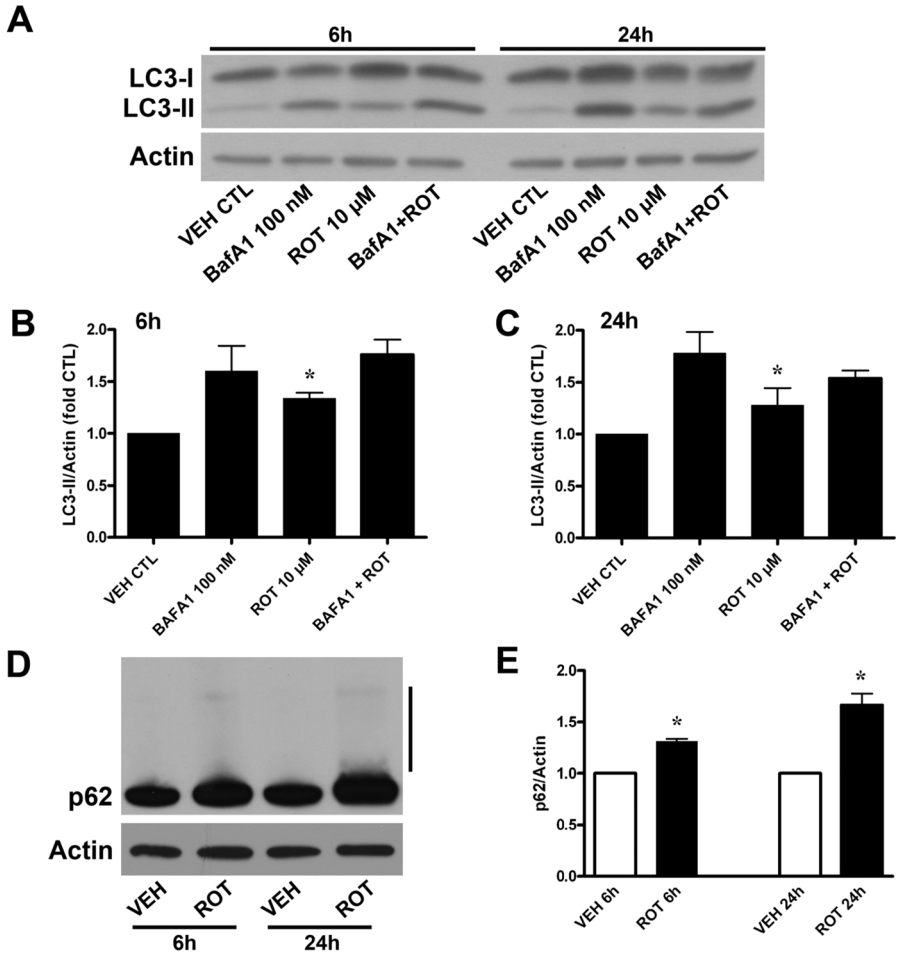

Figure 2. Rotenone causes accumulation of autophagic vacuoles by blocking their effective degradation. (A) Representative Western blot of LC3-II (14 kDa) and actin (42 kDa) loading control for SH-SY5Y lysates collected 6 and 24 h following treatment with 10 μM rotenone (ROT) in the presence or absence of 100 nM bafilomycin A1 (BafA1). Rotenone caused a significant increase in LC3-II immunoreactivity at both 6 and 24 h following treatment (A–C). To measure autophagic flux, 100nM BafA1 was added for the last 2 h of rotenone treatment prior to preparing lysates. Quantification of LC3-II/actin ratios for each treatment is expressed graphically as fold CTL for 6 h rotenone (B) and 24 h rotenone (C). Treatment with 10 μM rotenone induced a significant increase in AV accumulation, an effect that was not significantly greater upon treatment with 100 nM BafA1. Representative Western blot indicates that rotenone increase levels of the autophagy substrate p62 at both 6 and 24 h after treatment (D). Side bar in (D) indicates higher p62-immunoreactive species following 6 and 24 h treatment with rotenone that suggests its enhanced ubiquitination. Blots were stripped and reprobed for actin. Immunoreactivity for p62 (normalized to actin) is quantified graphically in (E) and is expressed as fold VEH CTL. Results = mean ± standard deviation from three to five independent experiments. *$p < 0.05$ vs VEH CTL.

Rotenone-induced SH-SY5Y cell death was accompanied by a concentration-dependent increase in caspase-3-like activity (Figure 1B). A 3- to 4-fold increase was also detected in caspase-3-like enzymatic activity in 10 μM rotenone treated SH-SY5Y cells versus vehicle control at 48 and 72 h, indicating that rotenone-induced cell death was accompanied by caspase activation (Figure 1D). All subsequent experiments utilized a concentration of 10 μM rotenone. To determine if caspase activation was required for rotenone-induced neuron death, we measured cell viability in the presence of a broad caspase inhibitor Boc-Asp(OMe)-FMK (Boc-FMK) (Figure 1E). Boc-FMK at a concentration that completely inhibited rotenone-induced caspase-3-like activity (data not shown) failed to inhibit rotenone-induced cell death. This data indicates that although rotenone can induce robust apoptosis, caspase activation, per se, is not required for cell death. To confirm that a death-inducing concentration of rotenone affected cellular energetic, ATP levels were measured at 6 and 12 h following rotenone treatment (Figure 1F), time points that preceded the induction of neuronal apoptosis and cell death (Figure 1C, D). Rotenone caused a significant reduction in ATP levels at both time points, due likely to the inhibition of complex I of the mitochondrial electron transport chain and indicates the reliance of these cells on mitochondrial ATP production as a source of energy.

Rotenone Causes Early and Persistent Accumulation of Autophagic Vacuoles by Compromising Their Lysosomal Degradation. Previous studies have identified accumulation of autophagic vacuoles in substantia nigra neurons of PD brain and in in vitro models of rotenone-induced neuronal cell death,[6−8,18,19,21] suggesting that the ALP is involved in regulating dopaminergic neuron death. To further delineate the involvement of macroautophagy in rotenone-induced neuronal cell death, we assessed levels of autophagic vacuoles via Western blot analysis for MAP-light chain 3-II (LC3-II; Figure 2), an accepted and selective marker of autophagic vacuoles.[3] Treatment with rotenone induced a significant accumulation of autophagic vacuoles at both 6 h (Figure 2B) and 24 h (Figure 2C) after treatment. Since the accumulation of autophagic vacuoles may result from either

dx.doi.org/10.1021/cn300145z | ACS Chem. Neurosci. 2012, 3, 1063−1072

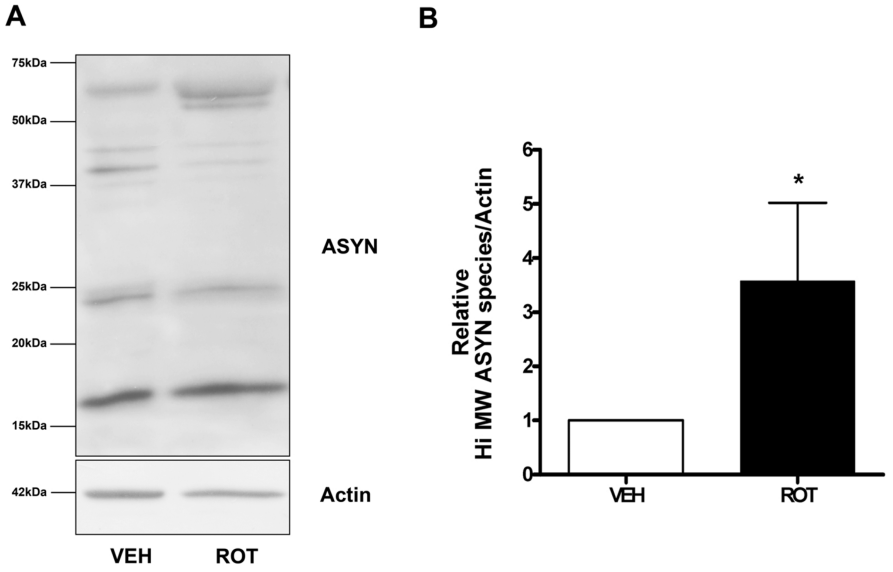

Figure 3. Rotenone increases levels of α-synuclein. (A) Representative Western blot analysis of whole cell lysates indicates an increase in high molecular weight species of α-synuclein (>50 kDa) following 48 h treatment with 10 μM rotenone. (B) Quantification of high-molecular weight species of α-synuclein indicates a significant increase vs vehicle control. Results = mean ± standard deviation obtained from three independent experiments. *p < 0.05 vs VEH CTL.

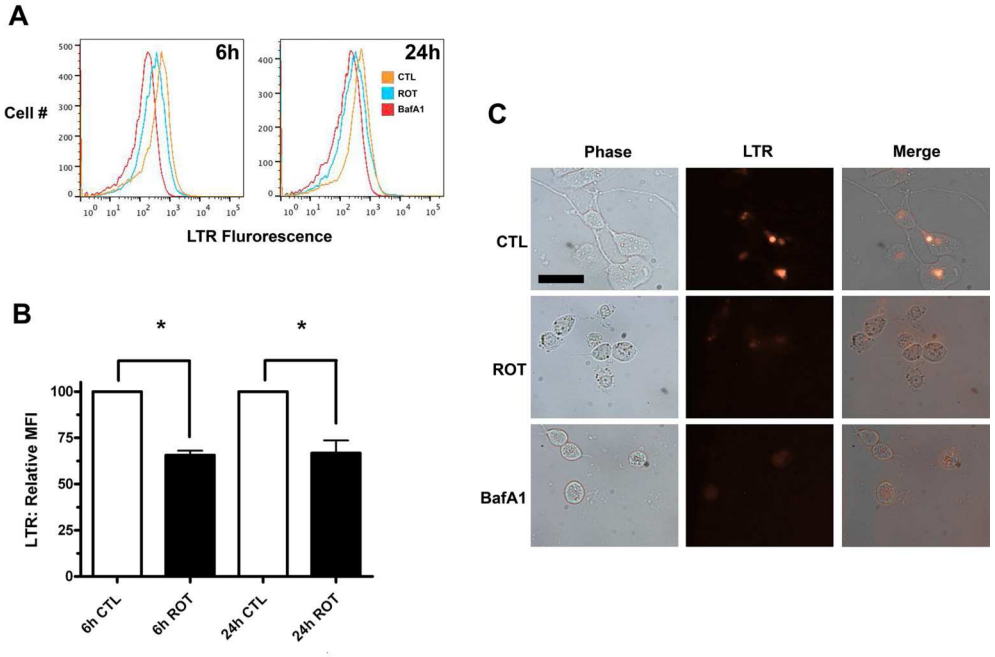

Figure 4. Rotenone causes an increase in acidic vesicle pH. (A) Representative histogram of alterations in acidic vesicle pH in SH-SY5Y cells after treatment with DMSO vehicle (VEH, 24 h, orange line), rotenone (ROT, 10 μM, 24 h, blue line), or bafilomycin A1 (BafA, 100 nM, 4 h, pink line) as determined by flow cytometry. Effects of rotenone treatment are expressed as a leftward shift in fluorescence in the cell population when compared to vehicle control, suggesting a loss of lysosomal/acidic vesicle pH. (B) Quantification of LTR mean fluorescence intensity (MFI) indicates a >30% decrease following 6 and 24 h treatment with rotenone. (C) Phase contrast and fluorescence microscopy were used to image the rotenone-induced attenuation of LTR fluorescence at 24 h after treatment. Results = mean ± standard deviation from five independent experiments. *p < 0.05 vs VEH CTL.

induction of autophagy or from a decrease in their lysosomal degradation[3,22] we also assessed autophagic flux (Figure 2) via treatment with 100 nM bafilomycin A1, a selective inhibitor of vacuolar-type V-ATPase that completely blocks degradation via macroautophagy through its inhibition of autophagic vacuole-lysosome fusion. Bafilomycin A1 was added to cells at 4 or 22 h (2 h prior to collection at the 6 and 24 h rotenone time points, respectively). At each time point tested, we found no further increase in levels of LC3-II in bafilomycin A1-rotenone-treated cells compared to cells treated only with 100 nM bafilomycin A1 (Figure 2B, C). This result suggests that the rotenone-induced increase in autophagic vacuoles resulted not from autophagy induction but rather from a block in the lysosomal degradation of autophagic vacuoles. As a positive control for

dx.doi.org/10.1021/cn300145z | ACS Chem. Neurosci. 2012, 3, 1063−1072

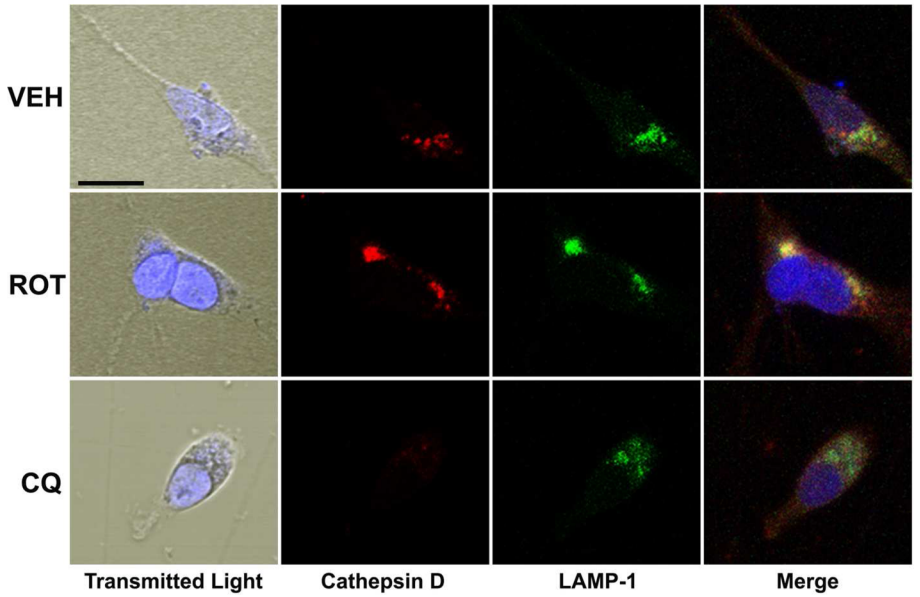

Figure 5. Rotenone does not induce lysosomal membrane permeabilization (LMP). Confocal microscopy images obtained via double label immunocytochemistry for the soluble lysosomal enzyme cathepsin D (red, Cy3) and the lysosomal membrane protein LAMP-1 (green, FITC) following treatment for 24 h with DMSO vehicle (top row), 10 μM rotenone (ROT, middle row), or 50 μM chloroquine (CQ, bottom row). Punctate immunoreactivity for cathepsin D that colocalized to regions of the cell exhibiting intense LAMP-1 immunoreactivity was apparent in vehicle and rotenone-treated cells. Diffuse staining for cathepsin D was observed in chloroquine-treated cells that did not localize intracellularly to that of LAMP-1, suggesting the onset of LMP. Images are representative of LMP assessment from three independent experiments.

autophagy induction, the addition of 100 nM BafA1 for the last 2 of a 24 h rapamycin treatment produced noticeably greater LC3-II immunoreactivity in comparison to 2 h treatment with BafA1 alone (data not shown).

Autophagic flux is also commonly assessed by detecting protein levels of p62/A170/SQSMT1, a ubiquinating and LC3 binding protein that binds to ubiquitin aggregates and promotes degradation via autophagy.[22] Thus, decreases in p62 levels are associated with enhanced autophagic flux as observed for example during serum starvation, whereas its accumulation suggests autophagy degradation block.[22] We observed a significant increase in p62 levels at both 6 h and 24 h following treatment with 10 μM rotenone (Figure 2D, E). These data support our assessment of autophagic flux (Figure 2A–C) suggesting that rotenone disrupts the degradation of autophagic vacuoles. Further evidence for rotenone-induced inhibition of autophagic degradation in our model was supported by a significant increase in high molecular weight species of α-synuclein at 48 h following treatment (Figure 3), as it is well established that the ALP is important for α-syn degradation.[8,23,24] Levels of alpha synuclein following 6 and 24 h of rotenone treatment were not significantly different from vehicle control (data not shown).

Rotenone Increases Acidic Vesicle pH but Does Not Induce Lysosomal Membrane Permeabilization. To determine if rotenone-induced inhibition of autophagic flux correlated with a compromise in the function of acidic vesicles, we utilized a flow cytometric approach with the acidotropic dye lysotracker red (LTR) to quantify acidic vesicle pH (Figure 4). Rotenone induced a significant, >30% loss in LTR mean fluorescence intensity versus vehicle control-treated cells at both 6 and 24 h following treatment, time points that coincided with the observed decrease in ATP production (6 h; Figure 1G) and inhibition of macroautophagy (Figure 2). The effects of rotenone on LTR mean fluorescence intensity were not as robust as those observed following treatment with 100 nM BafA1, a potent inhibitor of acidic vesicle pH via its direct inhibition of V-ATPase.[41] Epifluorescence microscopy images (Figure 4C) corroborate our findings via flow cytometry, where compared to vehicle-control-treated cells there is a relative lack of LTR fluorescence following treatment with rotenone or bafilomycin A1. These results indicate that rotenone causes an early and persistent increase in acidic vesicle pH, which may be due possibly to a net decrease in cellular ATP levels and in turn ATP-dependent acidification. Rotenone has been shown previously to inhibit cathepsin D activity and decrease fluorescence emitted by the acidotropic dye lysosensor green in cultured cell lines,[25,26] evidence that corroborates our findings.

We also determined if rotenone caused the onset of lysosomal membrane permeabilization (LMP) by assessing the colocalization of cathepsin D and LAMP-1 immunoreactivity using confocal microscopy (Figure 5). At 24 h after treatment with rotenone, a time point that corresponded to significant inhibition of autophagic flux (Figure 2), a significant decrease in LTR mean fluorescence intensity (Figure 4), and the onset of cell death/apoptosis (Figure 1), cathepsin D immunoreactivity colocalized with LAMP-1 similar to that of vehicle control-treated cells, suggesting a lack of LMP at this time point. In contrast, noticeable LMP (as indicated by a diffuse staining pattern for cathepsin D that did not colocalize with LAMP-1) was observed in cells treated for 24 h with chloroquine (50 μM; Figure 5), a lysosomotropic agent and known inducer of LMP.[27] Together these results suggest that the inhibition of autophagic flux by rotenone may be caused in part by its inhibition of vesicular acidification, perhaps via its potent inhibition of intracellular ATP, but not because of the onset of LMP. It is possible that rotenone may eventually induce LMP at later time points not tested in this study, as shown previously by the dopaminergic neurotoxin MPP+[9] and

dx.doi.org/10.1021/cn300145z | ACS Chem. Neurosci. 2012, 3, 1063–1072

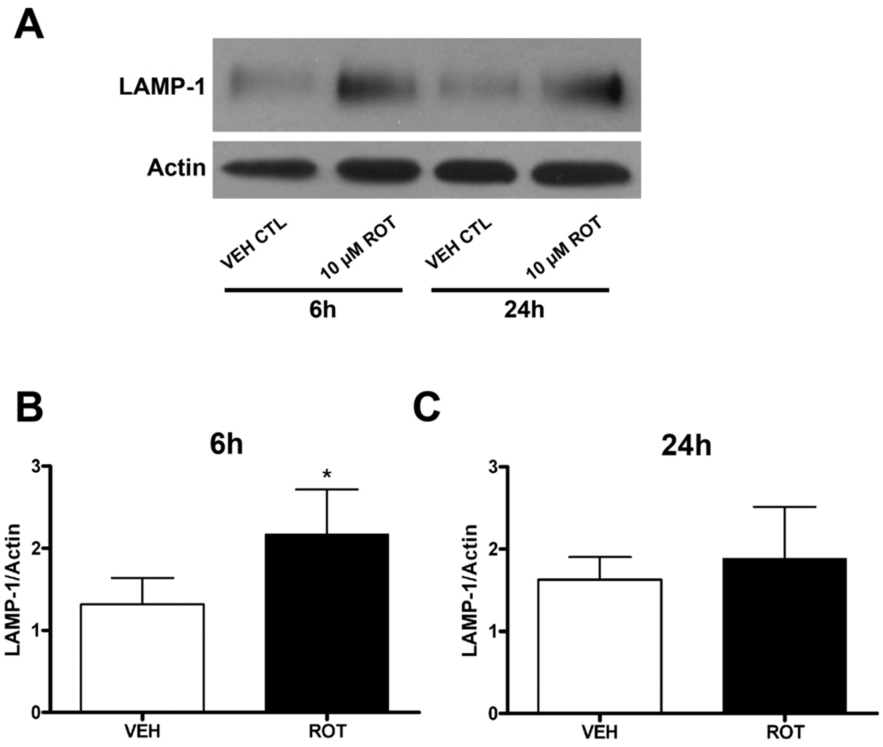

Figure 6. Rotenone increases levels of LAMP-1. Representative Western blot (A) for LAMP-1 (~110 kDa) along with actin (42 kDa) loading control for lysates obtained from SH-SY5Y cells treated with vehicle control (VEH CTL) or 10 μM rotenone (ROT) for 6 or 24 h. Quantification of LAMP-1 signal averaged from four independent experiments indicated that levels of LAMP-1 were significantly greater at 6 h following rotenone. *$p < 0.05$ vs vehicle CTL.

the oxidative stress-inducing agent hydrogen peroxide.[28] However, the possibility still exists that rotenone-induced oxidative stress in our model may compromise lysosomal membrane integrity that in turn may decrease the efficiency of macroautophagy for clearing substrates,[5] but at a lower concentration and earlier time than that is required for inducing LMP. Taken together, lysosome dysfunction corresponds with and may contribute to a decreased turnover of autophagic vacuoles following rotenone treatment, events that may be responsible for the accumulation of macroautophagy substrate and induction of cell death.

Rotenone Increased Levels of LAMP-1 but not TFEB. We also tested the effect of rotenone on levels of lysosomal membrane associated protein 1 (LAMP-1), a structural protein present on membranes of late endosomes and lysosomes. LAMP-1 is best known for its regulation of lysosomal motility and endosomal-lysosomal fusion with autophagic vacuoles,[29] and has been shown to fluctuate with changes in lysosomal volume and/or number.[9,30] Western blot analysis indicated an increase in LAMP-1 levels following treatment with 10 μM rotenone (Figure 6A), an effect that was significantly different vs vehicle control at 6 h but not 24 h (Figure 6B). This increase in LAMP-1-suggests an increase in either the number or size of acidic vesicles that may be a consequence of lysosome dysfunction (Figure 4) and inhibition of autophagic flux (Figure 2). Conversely, LAMP-1 may also increase as a function of de novo lysosome biogenesis, as shown recently under stressful conditions and as a response to alterations in autophagy.[9,30] To address this possibility the effects of rotenone on endogenous levels of the transcription factor EB (TFEB) were assessed by Western blot analysis, as TFEB has been shown previously to regulate transcription of LAMP-1 in addition to other lysosomal targets.[9,30] Levels of TFEB at 6 and 24 h following rotenone treatment were similar in rotenone vs vehicle control cells (Figure 7), suggesting that the increase in LAMP-1 observed following rotenone treatment does not result from lysosome biogenesis, but rather from the inhibition of lysosomal degradation.

Our assessment of autophagic flux suggests that induction of macroautophagy is not the major mechanism by which rotenone causes accumulation of autophagic vacuoles. In agreement with this interpretation, previous reports have shown that cell death and markers of apoptosis induced by 1−10 μM rotenone in SH-SY5Y are not influenced by siRNA knockdown of Atg5, a gene that is critical for de novo synthesis of autophagic vacuoles.[19,34] Interestingly, these studies also showed that pretreatment of SH-SY5Y cells with drugs that induce autophagy attenuate cell death and apoptosis caused by rotenone post-treatment.[19,34] These observations suggest that, in addition to its ability to block the lysosomal degradation of autophagic vacuoles, rotenone may also inhibit autophagy induction, an effect that is somehow circumvented upon pretreatment with drugs that stimulate formation of autophagic vacuoles. In support of this hypothesis, it has been shown that rotenone causes dephosphorylation of death-associated protein kinase (DAPK) in association with mitochondrial dysfunction.[35] The "active" phosphorylated form of DAPK has been shown to phosphorylate the BH3 domain of Beclin-1, thus disrupting the Bcl-XL-Beclin-1 interaction and in turn promoting Beclin-1-dependent autophagy.

Alternatively, it is possible that rotenone inhibits autophagy induction through its effects on microtubule assembly, as an intact microtubule network is also important for the formation of de novo autophagic vacuoles.[33,36] Rotenone has been shown

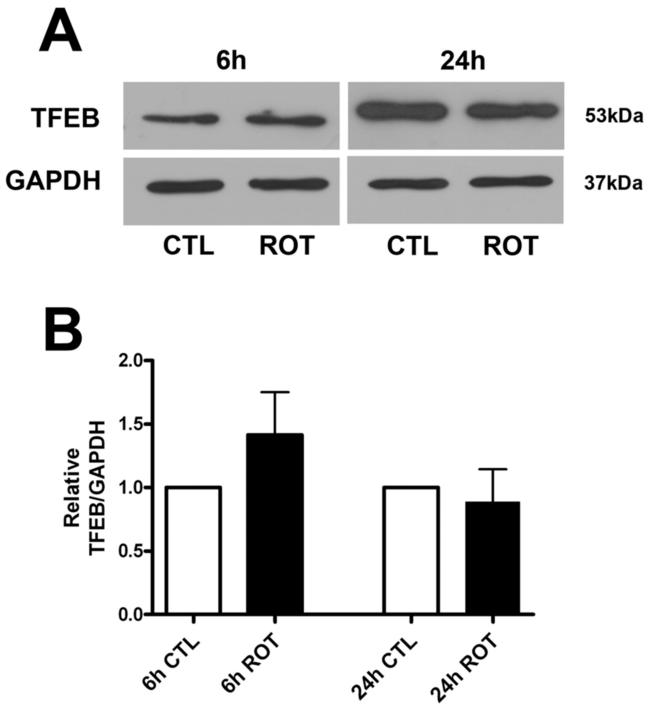

Figure 7. Rotenone exposure does not alter TFEB levels. (A) Representative Western blot analysis for TFEB (53 kDa) and GAPDH (37 kDa) loading control following 6 and 24 h treatment with vehicle control (CTL) or 10 μM rotenone (ROT). (B) Quantification of TFEB/GAPDH ratios following 6 and 24 h treatment of rotenone are expressed graphically as fold CTL. Results = mean ± standard deviation obtained from six independent experiments.

previously to inhibit microtubule assembly,[31] as well as increase levels of free tubulin in association with a decrease in mitochondrial membrane potential.[32] An intact microtubule network is known to be important not only for the formation of nascent autophagic vacuoles but also for the fusion of autophagic vacuoles with lysosomes and endosomes.[33] Thus, if rotenone disrupts the function of microtubules, it would not be surprising if autophagic vacuoles accumulate due to an effective block in their trafficking to lysosomes for degradation. Reduced turnover of autophagic vacuoles as a result of microtubule dysfunction may also contribute to persistent rotenone-induced mitochondrial toxicity, as the ability of damaged mitochondria to be effectively recycled by mitophagy (a type of macroautophagy selective for mitochondrial degradation) may be severely compromised.

Other reports indicate that rotenone exhibits concentration-specific or even cell type-specific effects on autophagy induction. Treatment of mouse embryonic fibroblasts with 2 μM rotenone caused accumulation of autophagic vacuoles concomitant with a reduction in levels of p62, suggesting autophagy induction.[21] Concurrent treatment of SH-SY5Y cells with 100 nM rotenone and either rapamycin, which induces autophagy, or 3-MA, which inhibits autophagy induction, attenuated or exacerbated cell death, respectively,[37] suggesting that autophagy induction is not inhibited by low concentrations of rotenone. In addition, inhibition of autophagy induction (3-MA vs Atg5 or Beclin-1 siRNA knockdown) in HEK 293 and U87 cells was shown to attenuate cell death induced by 50 μM rotenone,[18] suggesting again that rotenone does not inhibit autophagy induction and that autophagy induction may potentiate rotenone-induced cell death at higher concentrations. We have observed previously using knockdown of Atg7 that autophagy induction contributes to the onset of cell death induced by chloroquine, a lysosomotropic agent that inhibits autophagic flux,[38] suggesting that autophagy induction can be death-inducing in the face of lysosome dysfunction.

In conclusion, to our knowledge, this is the first report indicating that rotenone inhibits the lysosomal degradation of autophagic vacuoles. Inhibition of autophagic flux was observed at both early and late time points, and may be caused by the rotenone-induced increase in acidic vesicle pH and decrease in ATP levels. The induction of cell death and apoptosis was only apparent at later time points, suggesting that the inhibition of autophagic turnover by rotenone may contribute to cellular demise. In light of the relationship of rotenone as a neurotoxin model of PD, preservation and/or enhancement of autophagic degradation should be considered a viable therapeutic strategy to delay disease onset and/or progression.

METHODS

Cell Culture. SH-SY5Y human neuroblastoma cells were cultured in Minimum Essential Medium Eagle (MEM) (Cellgro, Herndon, VA) and F12-K Nutrient Mixture (ATCC, Manassas, VA) medium supplemented with 0.5% sodium pyruvate, 0.5% nonessential amino acids (Cellgro, Herndon, VA), 1% penicillin/streptomycin (Sigma, St. Louis, MO), and 10% fetal bovine serum (FBS) (HyClone, Logan, UT). SH-SY5Y cells were differentiated in 10% FBS feeding media supplemented with 10 μM retinoic acid (Sigma, St. Louis, MO) for 7−8 days. Medium supplemented with retinoic acid was replaced every 2−3 days. For experiments, cells were seeded at a density of 400/mm^2 in media containing 2% B-27 supplement (Invitrogen, Grand Island, NY) and 10 μM retinoic acid. Rotenone (Sigma, St. Louis, MO) stock in DMSO was prepared fresh for every experiment and added to differentiated SH-SY5Y cells for 3−72 h.

Measurement of Cell Viability and Caspase-3-like Activity. Cell viability was measured via Calcein AM fluorogenic conversion assay (Invitrogen, Grand Island, NY) and caspase-3-like activity was detected via fluorogenic DEVD cleavage assay and expressed relative to untreated controls as previously described in our laboratory.[39]

Measurement of ATP Levels. Differentiated SH-SY5Y cells were plated at 2 × 10^4 cells/well in 96-well plates and after 24 h were treated with either DMSO vehicle or rotenone at a final concentration of 10 μM. At 6 and 12 h following rotenone treatment, levels of ATP were assessed using the ATPLite Luminescence ATP Detection Assay System (Perkin-Elmer, Waltham, MA). Luminescence was quantified using a BioTek Synergy 2 luminometer. ATP levels (μM/well) were calculated based on a standard curve utilizing an ATP standard supplied by the assay kit. Mean ATP levels were averaged from six wells per treatment per time point, and each time point was repeated for a total of three independent experiments.

Western Blot Analysis. Whole cell lysates were prepared in buffer containing 1% SDS and 1% Triton X-100 as previously described in our laboratory.[40] Protein concentrations were determined using the BCA assay (Pierce, Rockford, IL). Equal amounts of protein were electrophoresed on SDS-polyacrylamide gels and subsequently transferred to PVDF membranes (BioRad, Hercules, CA). Western blots were probed for LC3 (Abcam, Cambridge, MA), p62 (Abnova, Littleton, CO), LAMP1 (1D4B; University of Iowa Hybridoma Bank), or α-synuclein (Santa Cruz, Santa Cruz, CA). GAPDH (Cell Signaling, Beverly, MA) or actin (Sigma, St. Louis, MO) was used as loading control. X-ray films of Western blots were scanned for densitometric analysis using UN-SCAN-IT gel 6.1 software (UN-SCAN-IT, Orem, UT).

Assessment of Lysosomal Membrane Permeabilization (LMP). To assess LMP, double-label immunocytochemistry was performed for cathepsin-D and LAMP-1. Cells plated in 8-well chamber slides were treated for 24 h with either DMSO vehicle, rotenone (10 μM), or chloroquine (50 μM) and then were fixed for 20 min with ice-cold 100% methanol. Following PBS wash, fixed cells

were incubated for 30 min with blocking buffer (5% v/v horse serum in 1× PBS containing 1% Triton X-100) followed by overnight incubation in blocking buffer without Triton X-100 and containing goat anti-cathepsin D antibody (Santa Cruz, Santa Cruz, CA). After PBS wash, cells were incubated in blocking buffer containing HRP-conjugated anti-goat IgG secondary antibody (ImmPRESS, Vector Laboratories, Burlingame, CA) for 1 h in the above blocking buffer, RT followed by PBS wash. Cells were next subjected to a second fixative (4% paraformaldehyde, 15 min, 4 °C) for 15 min to prevent membrane rupture that occurs following exposure of methanol-fixed cells to the high salt concentration of our detection reagent buffer. Following PBS wash, detection was performed using Tyramide Signal Amplification (TSA; Perkin-Elmer, Waltham, MA) by addition of Cy3-conjugated tyramide in Plus Amp Buffer (30 min, RT) followed by PBS wash. At this point, fixed cells were incubated in blocking buffer (1% BSA, 0.2% evaporated milk, 0.3% Triton X-100 in PBS) for 30 min at RT and then overnight in blocking buffer without Triton X-100 and containing the second primary antibody (mouse anti-human LAMP-1, U Iowa Hybridoma Bank). Following PBS wash, fixed cells were incubated with HRP-conjugated anti-mouse IgG secondary antibody (ImmPRESS, Vector Laboratories, Burlingame, CA). Following PBS wash, detection was performed via TSA upon addition of FITC-conjugated tyramide in Plus Amp Buffer (30 min, RT) followed by PBS wash. Nuclei were next counterstained using bis-benzimide (0.2 μg/mL, Sigma, St. Louis, MO) for 10 min, followed by PBS wash. After coverslipping, colocalization of cathepsin D and LAMP-1 was visualized using a Zeiss Observer.Z1 laser scanning microscope (Thornwood, NY) equipped with a Zeiss 40× 1.3 oil DIC M27 Plan-Apochromat objective and imaged using Zen 2008 LSM 710, V5.0 SP1.1 software. Transmitted light images were also taken using DIC optics. Fluorescence filters were used to observe bis-benzimide (excitation 405 nm, emission 409−514 nm), FITC (excitation 488 nm, emission 494−572 nm), and Cy3 (excitation 543 nm, emission 585−734 nm).

Measurement of Lysotracker Red Staining Intensity. Cells were plated at 1×10^6 cells/well in a 6-well dish and were treated with DMSO vehicle or rotenone (10 μM) for either 6 or 24 h, or bafilomycin A1 (100 nM) for 4 h prior to analysis by flow cytometry. Cells were then incubated with LysoTracker Red (100 nM final concentration, Life Technologies, Eugene, OR) in Locke's buffer (154 mM NaCl, 5.6 mM KCl, 3.6 mM $NaHCO_3$, 1.3 mM $CaCl_2$, 1 mM $MgCl_2$, 10 mM HEPES, 1.009 g/L glucose, pH 7.4) for 1 h. Cells were then harvested, pelleted, and resuspended in 1× PBS buffer before being passed through a 70 μm nylon cell strainer (BD Falcon, Durham, NC) into collection tubes to provide a single cell suspension. Cells were kept on ice and protected from light during immediate transport to the flow cytometry facility (Joint UAB Flow Cytometry Facility; Enid Keyser, Director) for analysis. A total of 1×10^4 events were detected in each experimental condition using the BD LSR II flow cytometer (Becton Dickinson, San Jose, CA). Further analysis was completed using FlowJo software (Ashland, OR, licensed by UAB). LTR fluorescence was also visualized via microscopy. Subets of cells were plated in 8 well glass chamber slides (Lab-Tek, Rochester, NY) at a density of 6×10^4 cells/well for treatment with vehicle or rotenone (24 h), or bafilomycin A1 (4 h). Following 1 h incubation, LTR was assessed via microscopy using a Zeiss Axioskop fluorescent microscope (Carl Zeiss Microimaging, LLC, Thornwood, NY) at 40× magnification using bis-benzimide (0.2 μg/mL) for nuclear counterstain. Transmitted light images were also taken using phase contrast optics. Representative images were collected using AxioVision 4.8 software (Carl Zeiss, Thornwood, NY).

Statistics. Significant effects of treatment were analyzed either by Student's t test (when two groups were being compared), by one-factor ANOVA (when effects of treatment or time were assessed across multiple groups, or by two-factor ANOVA (when the effects of time vs rotenone treatment were assessed). Post hoc analysis was conducted using Bonferroni's test. A level of $p < 0.05$ was considered significant.

AUTHOR INFORMATION

Corresponding Author

*Telephone: 205-996-7252. Fax: 205-934-6700. E-mail: shacka@uab.edu. Mailing address: Dept. Pathology, Neuropathology Division, University of Alabama at Birmingham, SC 930G4, 1530 3rd Ave. S, Birmingham, AL 35294.

Present Address

[§]Department of Neurology, University of Pittsburgh, Pittsburgh, PA.

Author Contributions

[‖]These authors contributed equally to this work.

Author Contributions

B.J.M., V.N.P., K.A.R., and J.J.S. conceived and directed the project. B.J.M., V.N.P., H.M.F., B.J.K., and L.R.M. performed experiments included in the manuscript. B.J.M., V.N.P., and J.J.S. drafted the manuscript. B.J.M., V.N.P., L.R.M., K.A.R., and J.J.S. edited the manuscript. All authors read and agreed on the final draft of the manuscript.

Funding

J.J.S. is supported by a VA Merit Award 1 I01 BX000957-01. K.A.R. is supported by NIH R01s (National NS35107, NS41962, and CA134773. We also thank the UAB Neuroscience Core facilities (NS047466 and NS057098) for technical assistance.

Notes

The authors declare no competing financial interest.

ACKNOWLEDGMENTS

We wish to thank Charles A. Taylor for expert technical support, and for Barry R. Bailey for expert administrative assistance in preparation of this manuscript.

REFERENCES

(1) Olanow, C. W., Stern, M. B., and Sethi, K. (2009) The scientific and clinical basis for the treatment of Parkinson disease (2009). *Neurology 72*, S1−136.

(2) Dauer, W., and Przedborski, S. (2003) Parkinson's disease: mechanisms and models. *Neuron 39*, 889−909.

(3) Klionsky, D. J., Abeliovich, H., Agostinis, P., Agrawal, D. K., Aliev, G., Askew, D. S., Baba, M., Baehrecke, E. H., Bahr, B. A., Ballabio, A., Bamber, B. A., Bassham, D. C., Bergamini, E., Bi, X., Biard-Piechaczyk, M., Blum, J. S., Bredesen, D. E., Brodsky, J. L., Brumell, J. H., Brunk, U. T., Bursch, W., Camougrand, N., Cebollero, E., Cecconi, F., Chen, Y., Chin, L. S., Choi, A., Chu, C. T., Chung, J., Clarke, P. G., Clark, R. S., Clarke, S. G., Clave, C., Cleveland, J. L., Codogno, P., Colombo, M. I., Coto-Montes, A., Cregg, J. M., Cuervo, A. M., Debnath, J., Demarchi, F., Dennis, P. B., Dennis, P. A., Deretic, V., Devenish, R. J., Di Sano, F., Dice, J. F., Difiglia, M., Dinesh-Kumar, S., Distelhorst, C. W., Djavaheri-Mergny, M., Dorsey, F. C., Droge, W., Dron, M., Dunn, W. A., Jr., Duszenko, M., Eissa, N. T., Elazar, Z., Esclatine, A., Eskelinen, E. L., Fesus, L., Finley, K. D., Fuentes, J. M., Fueyo, J., Fujisaki, K., Galliot, B., Gao, F. B., Gewirtz, D. A., Gibson, S. B., Gohla, A., Goldberg, A. L., Gonzalez, R., Gonzalez-Estevez, C., Gorski, S., Gottlieb, R. A., Haussinger, D., He, Y. W., Heidenreich, K., Hill, J. A., Hoyer-Hansen, M., Hu, X., Huang, W. P., Iwasaki, A., Jaattela, M., Jackson, W. T., Jiang, X., Jin, S., Johansen, T., Jung, J. U., Kadowaki, M., Kang, C., Kelekar, A., Kessel, D. H., Kiel, J. A., Kim, H. P., Kimchi, A., Kinsella, T. J., Kiselyov, K., Kitamoto, K., Knecht, E., Komatsu, M., Kominami, E., Kondo, S., Kovacs, A. L., Kroemer, G., Kuan, C. Y., Kumar, R., Kundu, M., Landry, J., Laporte, M., Le, W., Lei, H. Y., Lenardo, M. J., Levine, B., Lieberman, A., Lim, K. L., Lin, F. C., Liou, W., Liu, L. F., Lopez-Berestein, G., Lopez-Otin, C., Lu, B., Macleod, K. F., Malorni, W., Martinet, W., Matsuoka, K., Mautner, J., Meijer, A. J., Melendez, A., Michels, P., Miotto, G., Mistiaen, W. P., Mizushima, N.,

Mograbi, B., Monastyrska, I., Moore, M. N., Moreira, P. I., Moriyasu, Y., Motyl, T., Munz, C., Murphy, L. O., Naqvi, N. I., Neufeld, T. P., Nishino, I., Nixon, R. A., Noda, T., Nurnberg, B., Ogawa, M., Oleinick, N. L., Olsen, L. J., Ozpolat, B., Paglin, S., Palmer, G. E., Papassideri, I., Parkes, M., Perlmutter, D. H., Perry, G., Piacentini, M., Pinkas-Kramarski, R., Prescott, M., Proikas-Cezanne, T., Raben, N., Rami, A., Reggiori, F., Rohrer, B., Rubinsztein, D. C., Ryan, K. M., Sadoshima, J., Sakagami, H., Sakai, Y., Sandri, M., Sasakawa, C., Sass, M., Schneider, C., Seglen, P. O., Seleverstov, O., Settleman, J., Shacka, J. J., Shapiro, I. M., Sibirny, A., Silva-Zacarin, E. C., Simon, H. U., Simone, C., Simonsen, A., Smith, M. A., Spanel-Borowski, K., Srinivas, V., Steeves, M., Stenmark, H., Stromhaug, P. E., Subauste, C. S., Sugimoto, S., Sulzer, D., Suzuki, T., Swanson, M. S., Tabas, I., Takeshita, F., Talbot, N. J., Talloczy, Z., Tanaka, K., Tanida, I., Taylor, G. S., Taylor, J. P., Terman, A., Tettamanti, G., Thompson, C. B., Thumm, M., Tolkovsky, A. M., Tooze, S. A., Truant, R., Tumanovska, L. V., Uchiyama, Y., Ueno, T., Uzcategui, N. L., van der Klei, I., Vaquero, E. C., Vellai, T., Vogel, M. W., Wang, H. G., Webster, P., Wiley, J. W., Xi, Z., Xiao, G., Yahalom, J., Yang, J. M., Yap, G., Yin, X. M., Yoshimori, T., Yu, L., Yue, Z., Yuzaki, M., Zabirnyk, O., Zheng, X., Zhu, X., and Deter, R. L. (2008) Guidelines for the use and interpretation of assays for monitoring autophagy in higher eukaryotes. *Autophagy 4*, 151−175.

(4) Shacka, J. J., Roth, K. A., and Zhang, J. (2008) The autophagy-lysosomal degradation pathway: role in neurodegenerative disease and therapy. *Front. Biosci. 13*, 718−736.

(5) Pivtoraiko, V. N., Stone, S. L., Roth, K. A., and Shacka, J. J. (2009) Oxidative stress and autophagy in the regulation of lysosome-dependent neuron death. *Antioxid. Redox Signaling 11*, 481−496.

(6) Anglade, P., Vyas, S., Hirsch, E. C., and Agid, Y. (1997) Apoptosis in dopaminergic neurons of the human substantia nigra during normal aging. *Histol. Histopathol. 12*, 603−610.

(7) Zhu, J. H., Guo, F., Shelburne, J., Watkins, S., and Chu, C. T. (2003) Localization of phosphorylated ERK/MAP kinases to mitochondria and autophagosomes in Lewy body diseases. *Brain Pathol. 13*, 473−481.

(8) Yu, W. H., Dorado, B., Figueroa, H. Y., Wang, L., Planel, E., Cookson, M. R., Clark, L. N., and Duff, K. E. (2009) Metabolic activity determines efficacy of macroautophagic clearance of pathological oligomeric alpha-synuclein. *Am. J. Pathol. 175*, 736−747.

(9) Dehay, B., Bove, J., Rodriguez-Muela, N., Perier, C., Recasens, A., Boya, P., and Vila, M. (2010) Pathogenic lysosomal depletion in Parkinson's disease. *J. Neurosci. 30*, 12535−12544.

(10) Rubinsztein, D. C. (2006) The roles of intracellular protein-degradation pathways in neurodegeneration. *Nature 443*, 780−786.

(11) Betarbet, R., Sherer, T. B., MacKenzie, G., Garcia-Osuna, M., Panov, A. V., and Greenamyre, J. T. (2000) Chronic systemic pesticide exposure reproduces features of Parkinson's disease. *Nat. Neurosci. 3*, 1301−1306.

(12) Lai, B. C., Marion, S. A., Teschke, K., and Tsui, J. K. (2002) Occupational and environmental risk factors for Parkinson's disease. *Parkinsonism Relat. Disord. 8*, 297−309.

(13) Sherer, T. B., Betarbet, R., Testa, C. M., Seo, B. B., Richardson, J. R., Kim, J. H., Miller, G. W., Yagi, T., Matsuno-Yagi, A., and Greenamyre, J. T. (2003) Mechanism of toxicity in rotenone models of Parkinson's disease. *J. Neurosci. 23*, 10756−10764.

(14) Lee, H. J., and Lee, S. J. (2002) Characterization of cytoplasmic alpha-synuclein aggregates. Fibril formation is tightly linked to the inclusion-forming process in cells. *J. Biol. Chem. 277*, 48976−48983.

(15) Mirzaei, H., Schieler, J. L., Rochet, J. C., and Regnier, F. (2006) Identification of rotenone-induced modifications in alpha-synuclein using affinity pull-down and tandem mass spectrometry. *Anal. Chem. 78*, 2422−2431.

(16) Conway, K. A., Rochet, J. C., Bieganski, R. M., and Lansbury, P. T., Jr. (2001) Kinetic stabilization of the alpha-synuclein protofibril by a dopamine-alpha-synuclein adduct. *Science 294*, 1346−1349.

(17) Cole, N. B., Murphy, D. D., Lebowitz, J., Di Noto, L., Levine, R. L., and Nussbaum, R. L. (2005) Metal-catalyzed oxidation of alpha-synuclein: helping to define the relationship between oligomers, protofibrils, and filaments. *J. Biol. Chem. 280*, 9678−9690.

(18) Chen, Y., Millan-Ward, E., Kong, J., Israels, S. J., and Gibson, S. B. (2007) Mitochondrial electron-transport-chain inhibitors of complexes I and II induce autophagic cell death mediated by reactive oxygen species. *J.Cell Sci. 120*, 4155−4166.

(19) Pan, T., Rawal, P., Wu, Y., Xie, W., Jankovic, J., and Le, W. (2009) Rapamycin protects against rotenone-induced apoptosis through autophagy induction. *Neuroscience 164*, 541−551.

(20) Wu, Y., Li, X., Xie, W., Jankovic, J., Le, W., and Pan, T. (2010) Neuroprotection of deferoxamine on rotenone-induced injury via accumulation of HIF-1 alpha and induction of autophagy in SH-SY5Y cells. *Neurochem. Int. 57*, 198−205.

(21) Tang, D., Kang, R., Livesey, K. M., Kroemer, G., Billiar, T. R., Van Houten, B., Zeh, H. J., 3rd, and Lotze, M. T. (2011) High-mobility group box 1 is essential for mitochondrial quality control. *Cell Metab. 13*, 701−711.

(22) Mizushima, N., Yoshimori, T., and Levine, B. (2010) Methods in mammalian autophagy research. *Cell 140*, 313−326.

(23) Lee, H. J., Khoshaghideh, F., Patel, S., and Lee, S. J. (2004) Clearance of alpha-synuclein oligomeric intermediates via the lysosomal degradation pathway. *J. Neurosci. 24*, 1888−1896.

(24) Ruan, Q., Harrington, A. J., Caldwell, K. A., Caldwell, G. A., and Standaert, D. G. (2010) VPS41, a protein involved in lysosomal trafficking, is protective in Caenorhabditis elegans and mammalian cellular models of Parkinson's disease. *Neurobiol. Dis. 37*, 330−338.

(25) Wang, A. L., Lukas, T. J., Yuan, M., Du, N., Tso, M. O., and Neufeld, A. H. (2009) Autophagy and exosomes in the aged retinal pigment epithelium: possible relevance to drusen formation and age-related macular degeneration. *PLoS One 4*, e4160.

(26) Yong-Kee, C. J., Sidorova, E., Hanif, A., Perera, G., and Nash, J. E. (2012) Mitochondrial Dysfunction Precedes Other Sub-Cellular Abnormalities in an In Vitro Model Linked with Cell Death in Parkinson's Disease. *Neurotox Res. 21*, 185−194.

(27) Boya, P., Gonzalez-Polo, R. A., Poncet, D., Andreau, K., Vieira, H. L., Roumier, T., Perfettini, J. L., and Kroemer, G. (2003) Mitochondrial membrane permeabilization is a critical step of lysosome-initiated apoptosis induced by hydroxychloroquine. *Oncogene 22*, 3927−3936.

(28) Boya, P., and Kroemer, G. (2008) Lysosomal membrane permeabilization in cell death. *Oncogene 27*, 6434−6451.

(29) Saftig, P., Schroder, B., and Blanz, J. (2010) Lysosomal membrane proteins: life between acid and neutral conditions. *Biochem. Soc. Trans. 38*, 1420−1423.

(30) Sardiello, M., Palmieri, M., di Ronza, A., Medina, D. L., Valenza, M., Gennarino, V. A., Di Malta, C., Donaudy, F., Embrione, V., Polishchuk, R. S., Banfi, S., Parenti, G., Cattaneo, E., and Ballabio, A. (2009) A gene network regulating lysosomal biogenesis and function. *Science 325*, 473−477.

(31) Brinkley, B. R., Barham, S. S., Barranco, S. C., and Fuller, G. M. (1974) Rotenone inhibition of spindle microtubule assembly in mammalian cells. *Exp. Cell Res. 85*, 41−46.

(32) Ren, Y., Liu, W., Jiang, H., Jiang, Q., and Feng, J. (2005) Selective vulnerability of dopaminergic neurons to microtubule depolymerization. *J. Biol. Chem. 280*, 34105−34112.

(33) Kochl, R., Hu, X. W., Chan, E. Y., and Tooze, S. A. (2006) Microtubules facilitate autophagosome formation and fusion of autophagosomes with endosomes. *Traffic 7*, 129−145.

(34) Filomeni, G., Graziani, I., De Zio, D., Dini, L., Centonze, D., Rotilio, G., and Ciriolo, M. R. (2012) Neuroprotection of kaempferol by autophagy in models of rotenone-mediated acute toxicity: possible implications for Parkinson's disease. *Neurobiol. Aging 33*, 767−785.

(35) Shang, T., Joseph, J., Hillard, C. J., and Kalyanaraman, B. (2005) Death-associated protein kinase as a sensor of mitochondrial membrane potential: role of lysosome in mitochondrial toxin-induced cell death. *J. Biol. Chem. 280*, 34644−34653.

(36) Aplin, A., Jasionowski, T., Tuttle, D. L., Lenk, S. E., and Dunn, W. A., Jr. (1992) Cytoskeletal elements are required for the formation and maturation of autophagic vacuoles. *J. Cell. Physiol. 152*, 458−466.

(37) Dadakhujaev, S., Noh, H. S., Jung, E. J., Cha, J. Y., Baek, S. M., Ha, J. H., and Kim, D. R. (2010) Autophagy protects the rotenone-

induced cell death in alpha-synuclein overexpressing SH-SY5Y cells. *Neurosci. Lett. 472*, 47−52.
(38) Walls, K. C., Ghosh, A. P., Franklin, A. V., Klocke, B. J., Ballestas, M., Shacka, J. J., Zhang, J., and Roth, K. A. (2010) Lysosome dysfunction triggers Atg7-dependent neural apoptosis. *J. Biol. Chem. 285*, 10497−10507.
(39) Shacka, J. J., Klocke, B. J., Shibata, M., Uchiyama, Y., Datta, G., Schmidt, R. E., and Roth, K. A. (2006) Bafilomycin A1 inhibits chloroquine-induced death of cerebellar granule neurons. *Mol. Pharmacol. 69*, 1125−1136.
(40) Pivtoraiko, V. N., Harrington, A. J., Mader, B. J., Luker, A. M., Caldwell, G. A., Caldwell, K. A., Roth, K. A., and Shacka, J. J. (2010) Low-dose bafilomycin attenuates neuronal cell death associated with autophagy-lysosome pathway dysfunction. *J. Neurochem. 114*, 1193−1204.
(41) Bowman, E. J., Siebers, A., and Altendorf, K. (1988) Bafilomycins: a class of inhibitors of membrane ATPases from microorganisms, animal cells, and plant cells. *Proc. Natl. Acad. Sci. U.S.A. 85*, 7972−7976.